Aalborg Universitet

AALBORG UNIVERSITY
DENMARK

Reactive Power Impact on Lifetime Prediction of Two-level Wind Power Converter

Zhou, Dao; Blaabjerg, Frede; Lau, M.; Tonnes, M.

Published in:
Proceedings of PCIM Europe 2013

Publication date:
2013

Link to publication from Aalborg University

Citation for published version (APA):
Zhou, D., Blaabjerg, F., Lau, M., & Tonnes, M. (2013). Reactive Power Impact on Lifetime Prediction of Two-level Wind Power Converter. In *Proceedings of PCIM Europe 2013* (pp. 564-571). VDE Verlag GMBH.

Reactive Power Impact on Lifetime Prediction
of Two-level Wind Power Converter

D. Zhou[1,2], F. Blaabjerg[1], M. Lau[2], M. Tonnes[2]

[1] Aalborg University, Pontoppidanstraede 101,DK-9220 Aalborg, Denmark

[2] Danfoss Silicon Power GmbH, Husumer Strasse 251, D-24941 Flensburg, Germany

Abstract

The influence of reactive power injection on the dominating two-level wind power converter is investigated and compared in terms of power loss and thermal behavior. Then the lifetime of both the partial-scale and full-scale power converter is estimated based on the widely used Coffin-Manson model. It is concluded that the injection of the reactive power could have serious impact on the power loss and thermal profile, especially at lower wind speed. Furthermore, the introduction of the reactive power could also shorten the lifetime of the wind power converter significantly.

1.   Introduction

The penetration of wind power is expected to achieve 20% of the total electricity production by 2020 in Europe [1]. Because of the noise emission, land limits and richer wind energy, the wind turbines are moving from onshore to offshore. Meanwhile, the lifetime of the wind turbine system are inversely prolonged to 20-25 years under such uncertain and harsh environment, whose mission profile leads to a faster fatigue and higher failure rate. As the most vulnerable power electronic component, more and more efforts have been devoted to the reliable behavior of the power semiconductor recently due to the increased cost and time for repair after failures [2]-[4].

Fig. 1.   Active/reactive power operation range of offshore wind farm defined by E.on-Netz [5]

A large number of wind farms are increasing being installed in terminal of the power transmission system. The weak connections demand the ability of reactive power supply in order

to support the voltage regulation (e.g. the active/reactive power requirement [5] for offshore wind power application issued by German transmission system operator).

The scope of this paper is first to analyze the effects of the reactive power based on commonly used partial-scale and full-scale wind power systems. Then the power loss and thermal behavior of the power device are mapped and compared in terms of whether reactive power is injected or not. Finally, the lifetime expectancy of the power semiconductor, which is closely related to the thermal profile, is estimated based on an annual wind profile.

2. Effect of reactive power on typical topologies

Due to extensive and well-established knowledge, as well as the simper structure and fewer components, the two-level back-to-back power converter is the most attractive solution in commercial market of wind turbines [6]. The utilization of power electronics in wind turbine system can be further divided into two categories, namely: Doubly Fed Induction Generator (DFIG) system based partial-scale power converter and Permanent Magnet Synchronous Generator (PMSG) system based full-scale power converter, which are both illustrated in Fig. 2.
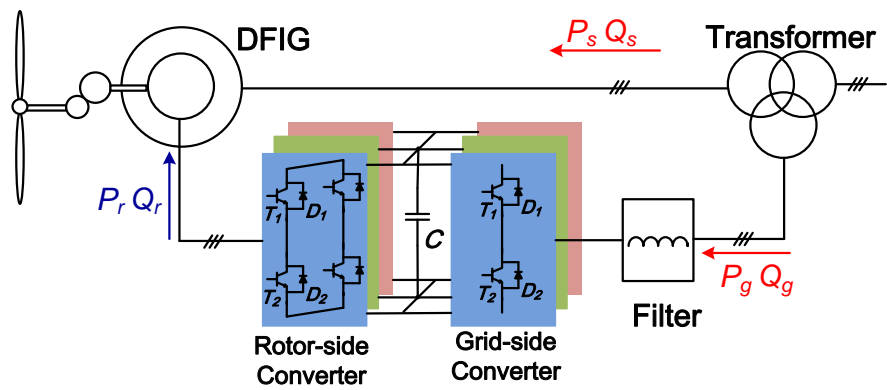
(a) DFIG-based partial-scale topology (with gearbox).
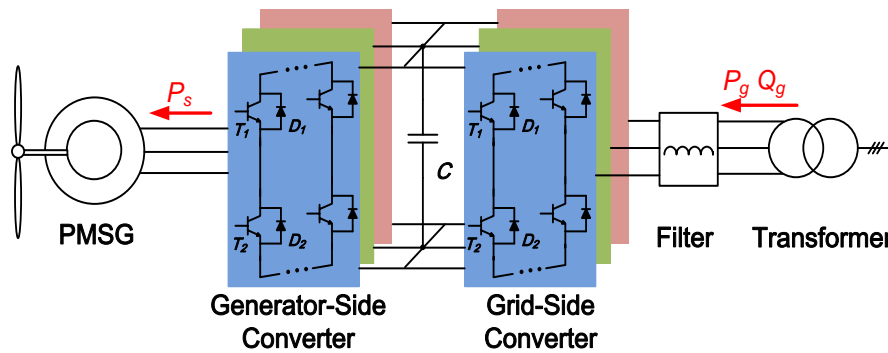
(b) PMSG-based full-scale topology (directly-drive).

Fig. 2. State-of-the-art configurations for two-level wind turbine system

For case study, Table 1 summarizes the relevant parameters of a 2 MW DFIG-based and PMSG-based wind turbine systems. As shown in Fig. 2(a), due to the dual links to the power grid in terms of the induction generator's stator and the partial-scale back-to-back power converter, there are two possibilities to compensate the reactive power by Q_g from the Grid-Side Converter (GSC) and Q_s from the Rotor-Side Converter (RSC). Consequently, it is interesting to investigate and compare the effects of these two compensation approaches on the performance of the power converter.

Table 1: Parameters for 2 MW DFIG & PMSG Wind Turbine Systems

	DFIG system	PMSG system
Power converter's rated Power P_g	330 kW	2000 kW
Rated grid phase voltage U_{gm}	564 V	564 V
DC-link voltage U_{dc}	1050 V	1100 V
Filter inductance L_g	0.5 mH	0.15 mH
Stator inductance L_s	2.94 mH	0.276 mH
Magnetizing inductance L_m	2.91 mH	
Rotor inductance L_r	2.97 mH	/
GSC and RSC switching freq. f_s	2 kHz	2 kHz
Power device in each GSC cell	1 kA/1.7 kV, single	1 kA/1.7 kV, four in paralleled
Power device in each RSC cell	1 kA/1.7 kV, two in paralleled	1 kA/1.7 kV, four in paralleled

If the reactive power is compensated from the RSC, owing to current limitation from power semiconductor, the rotor current will be,

$$k\sqrt{\frac{4}{9}\frac{X_s^2}{X_m^2 U_{gm}^2}(P_s^2+Q_s^2)-\frac{4}{9}\frac{X_s}{X_m^2}Q_s+\frac{U_{gm}^2}{X_m^2}} \le 2I_m$$

(1)

where k denotes the generator's stator/rotor turns ratio, X_s, X_m, X_r denote stator reactance, magnetizing reactance and rotor reactance, all of which are consistent with the Table 1, I_m denotes the current capacity of a single power device.

Furthermore, the line-to-line rotor voltage amplitude cannot exceed DC-link voltage restricted by the linear modulation range,

$$\frac{|s|}{k}\sqrt{\frac{4}{9}(\frac{\sigma X_r X_s}{X_m U_{sm}})^2(P_s^2+Q_s^2)-\frac{4}{9}\frac{\sigma X_r X_s}{X_m U_{sm}}Q_s+(\frac{X_r U_{sm}}{X_m})^2} \le \frac{U_{dc}}{\sqrt{3}}$$

(2)

where s denotes slip value, σ denotes leakage factor of the induction generator, U_{dc} denotes the DC-link voltage.

Since the wind speed at 10 m/s is regarded as one of the highest probability among offshore wind speed distribution [7], the influence of the reactive power injection upon back-to-back power converter will be focused under this circumstance.

Substituting the parameter values indicated in Table 1, the range of reactive power from the RSC will satisfy the E.on-Netz requirement.

Similarly, if the reactive power is injected from the GSC, the converter's out current and voltage will be expressed like (3), (4), which is also restricted by power device current rating and linear modulation,

$$\sqrt{\frac{4}{9}\frac{P_g^2+Q_g^2}{U_{gm}^2}} \le I_m$$

(3)

$$\sqrt{(U_{gm}-\frac{2X_g}{3U_{gm}}Q_g)^2+(\frac{2X_g}{3U_{gm}}P_g)^2} \le \frac{U_{dc}}{\sqrt{3}}$$

(4)

Due to the DC-link limitation, the reactive power range is from 0.3 p.u. under-excited to 0.1 p.u. over-excited. As a result, the grid code on reactive requirement fails to meet, which also means the GSC require a higher DC-link voltage than the RSC in condition of the same amount of the over-excited reactive power.


(a) Device loading vs. reactive power Q   (b) Phase angle vs. reactive power Q
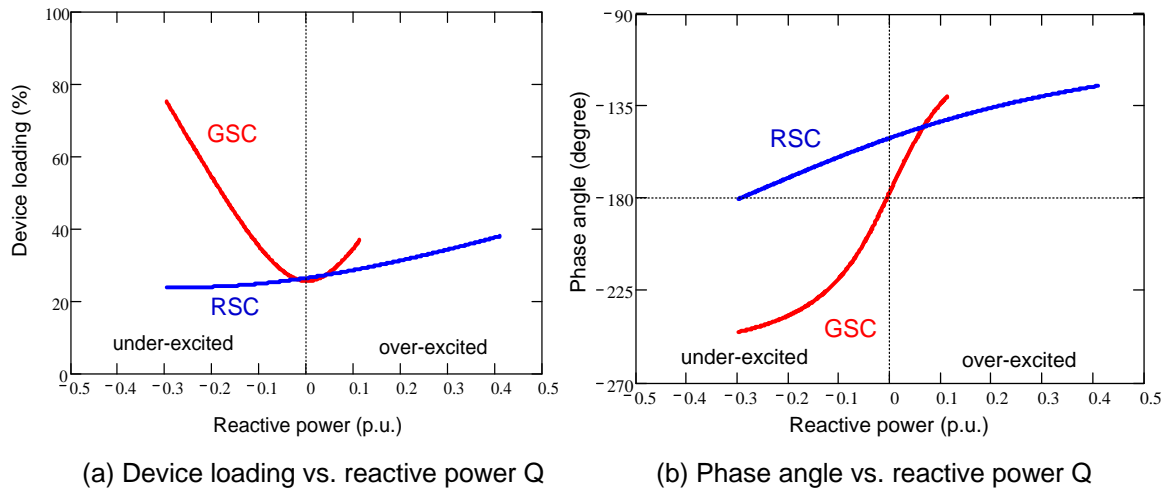
Fig. 3. Current characteristic of back-to-back power converter in a DFIG system (wind speed: 10 m/s)

The current characteristic of the back-to-back power converter in the DFIG system is illustrated in Fig. 3. For the characteristic of the device loading, it is clearly noted that the current will increase obviously in conditions of either under-excited or over-excited injection from the GSC, while the current will only change a little bit and even decrease in case of the under-excited reactive power injection, because the additional reactive power demand for grid code can contribute to the excitation of the induction generator. For the characteristic of power factor angle, for the GSC, it is noted that, in response to the additional reactive power injection, unity power factor easily becomes either leading or lagging power factor. For the RSC, it is noted that the phase shift looks insignificant.

For the PMSG system illustrated in Fig. 2(b), the reactive power compensation can only be fed through the GSC. It shares the same analysis criteria referred to the GSC in the DFIG system.

## 3.   Loss distribution considering grid codes

The power loss model, consisting of the conduction losses and switching losses, can be referred to [8]. Based on the on-state voltage drop and switching energy against the load current and the DC-link voltage provided by the manufacturers, the conduction losses and switching losses are accumulated by every switching cycle within one fundamental frequency. The simulation of the power loss has been realized according to PLECS block in Simulink [9].

(a)   (b)
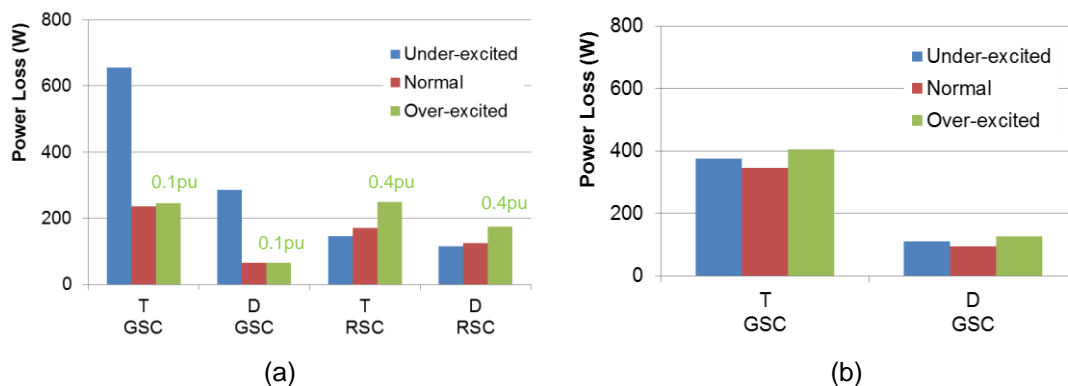
Fig. 4. Loss distribution of each power device with extreme amount reactive power (a) Grid-side converter and rotor-side converter in a DFIG-based system. (b) Grid-side converter in a PMSG-based system. (wind speed: 10 m/s)

The analysis about the loss distribution of each power semiconductor with extreme amount of reactive power is shown in Fig. 4. For the DFIG system, the same amount of the reactive power injection from the RSC will have a slighter impact on the power loss than the GSC. Moreover, it will even reduce the power loss in case of the under-excited reactive current, which is consistent with above mentioned current characteristic analysis. Therefore, it is better to compensate the reactive power from the RSC. For the PMSG system, the injection of both under-excited and over-excited reactive power will increase the power loss insignificantly.

In order to evaluate the influence of the reactive power upon the power semiconductor among the whole operational wind range, Fig. 5 shows the generator's output power and turbine speed against wind speed of the wind power generation system. For the DFIG system, as stated in [8], the synchronous operation of the doubly-fed induction generator will induce the extremely unbalanced power device loading among the three-phase bridge in the RSC. As a result, a small turbine speed hysteresis is introduced for minimum rotor frequency 1 Hz.
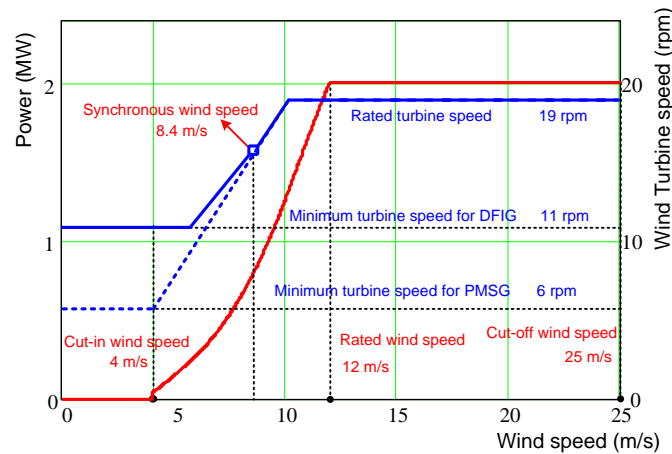
Fig. 5. Output power and turbine speed against wind speed

Accordingly, as shown in Fig. 6, the loss distribution of each power converter under the whole wind speed operation is mapped in conditions of over-excited, normal and under-excited reactive power requirements, where the reactive power is fed through RSC in the DFIG system and through GSC in the PMSG system. It can be seen that the power loss increase with the higher wind speed continuously in both systems. Moreover, it is evident that the reactive power influence to power loss is more serious in the DFIG than the PMSG system, and the reactive power introduces more additional power loss in condition of lower wind speed.
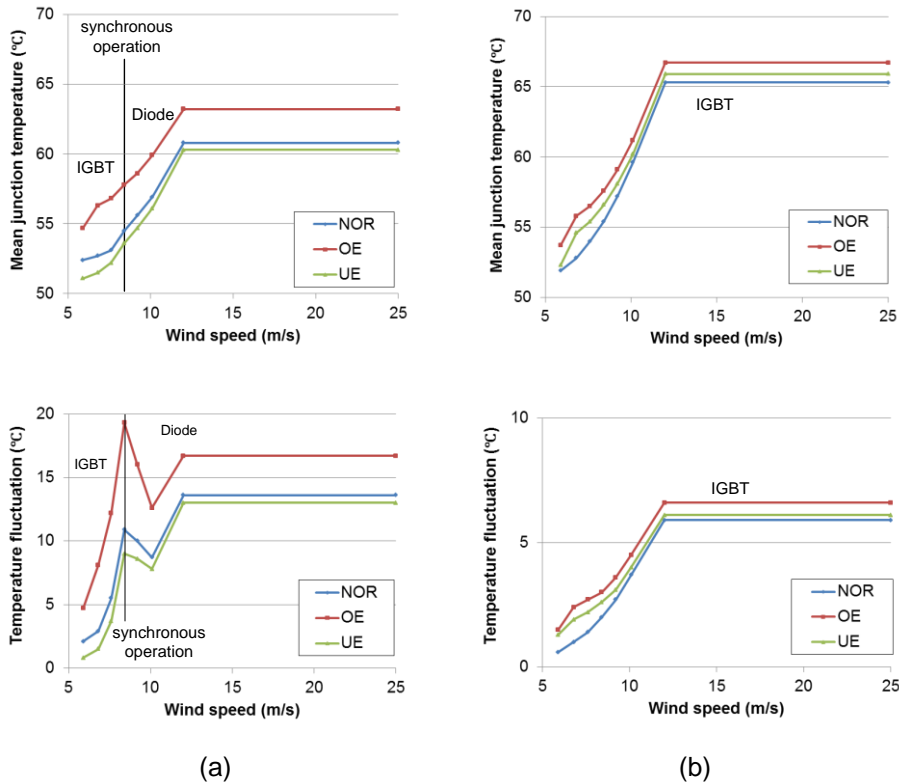

(a)

(b)
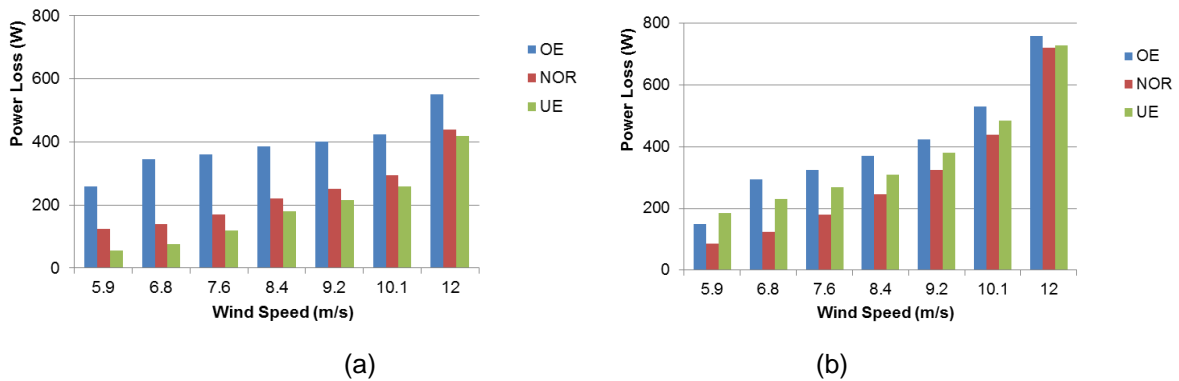
Fig. 6. Loss distribution of each power converter under the whole wind speed operation (a) Rotor-side converter in a DFIG-based system. (b) Grid-side converter in a PMSG-based system.

4. Thermal distribution considering grid codes

The one-dimensional thermal model of single IGBT and freewheeling diode share the same idea as discussed in [10]. With the aid of the previous power loss results, the junction temperature can be again simulated using PLECS-software. As the most stressed power semiconductor decides the reliability and lifetime in a power module, it is necessary to extract the thermal excursion of the most serious loading chips in both the DFIG and PMSG system considering the grid codes.

For the RSC of the DFIG system as shown in Fig. 7 (a), the most stressed power semiconductor changes from the IGBT in sub-synchronous mode to the freewheeling diode in super-synchronous mode. It is also noted that the over-excited reactive power requirement will impose thermal stress to the power semiconductor especially at synchronous operating point. For the GSC of the PMSG system as shown in Fig. 7(b), the IGBT is the most stressed power semiconductor during the whole operating wind speed. The reactive power injection will induce higher mean junction temperature and junction temperature fluctuation. Moreover, the situation will become worse at lower wind speed due to the lower output active power but the same amount of the reactive power is demanded.

(a)   (b)

Fig. 7. Mean junction temperature and temperature fluctuation in the chip vs. wind speed for both systems. (a) Rotor-side converter in a DFIG-based system. (b) Grid-side converter in a PMSG-based system.

5. Lifetime estimation

The junction temperature excursion of the power semiconductor is the most dominant reason for failure mechanisms, e.g. wire bonds lift-off, solder joint of chips cracking and solder joint of conductor leads cracking [11], [12]. Hence, it is interesting to investigate the correlations between lifetime of a module and the thermal stress. One of the commonly accepted models is known as the Coffin-Manson formula,

$$N_f = A\left(\Delta T\right)^{\alpha} \cdot \exp(\frac{E_a}{k_b \cdot T_m})$$

(5)

where the junction temperature swing ΔT and mean temperature T_m are taken into consideration, and A, α can be obtained by experimental measurements. Moreover, E_a and k_b denote activation energy and Boltzman constant, respectively.

Based on the power cycle test data of B10 lifetime (the number of cycles during which 10% of the total number of modules fail), the curves of power cycle with different temperature swings as well as mean temperatures are shown in Fig. 8, where the above mentioned model can fit the testing data well. Therefore, it can be extrapolated to the whole temperature variation range.
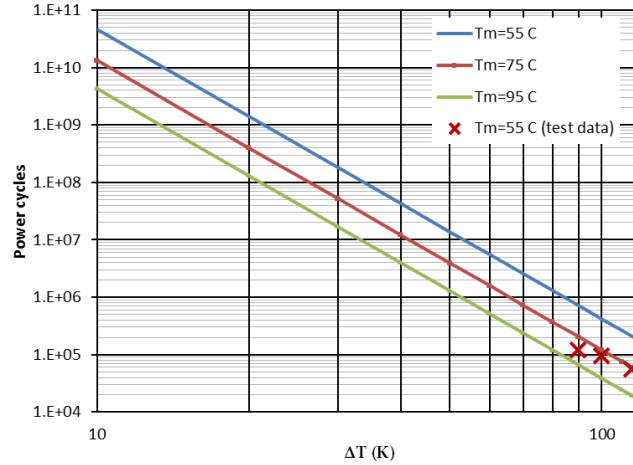

Fig. 8. B10 lifetime curve as a function of temperature swing and mean temperature

Many test results also indicate that time pulse duration t_{on} will have a considerable impact on the power cycles. It is assumed that a given number of power cycles N_{test} is tested at duration T_{on_test}. If the power modules are used for a different application with pulse duration T_{on_app}, the new power cycles N_{app} will equal to,

$$N_{app} = N_{test} (\frac{T_{on\_app}}{T_{on\_test}})^{\beta} \tag{6}$$

where β can be obtained according to the test experience.

(a)   (b)
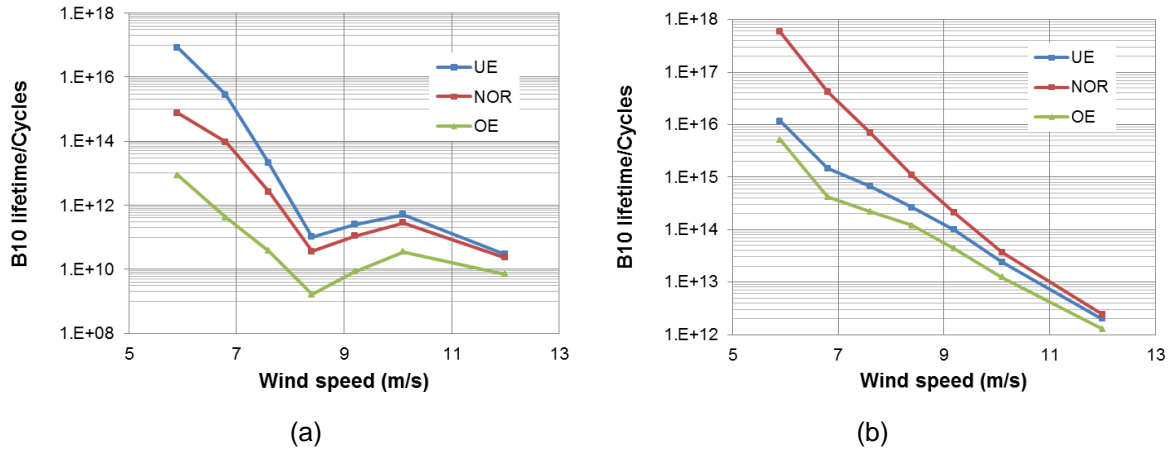
Fig. 9. Power cycle/B60 lifetime of the both systems. (a) Rotor-side converter in a DFIG-based system. (b) Grid-side converter in a PMSG-based system.

The effects of the reactive power injection to power cycle lifetime can be calculated at whole wind speed operation as shown in Fig. 9 in terms of the two dominating wind turbine systems. For the DFIG system, under-excited reactive power injection can contribute to the power converter's lifetime en-

hancement. Moreover, although the mean junction temperature increases with the wind speed, during synchronous operation the power cycles become extremely lower due to the higher junction temperature fluctuation. For the PMSG system, the wind system operation without reactive power injection has the highest power cycles, which is consistent with the thermal information indicated in Fig. 7(b).

With the typical wind profile as well as the Palmgren-Miner law [13], it can be inferred that, if the reactive power is introduced by grid codes, for the DFIG system, the lifetime of the RSC reduces from 498 to 102 years, while for the PMSG system, the lifetime of GSC varies from 11609 to 5785 years.

6. Conclusion

In this paper, the effect of reactive power on typical wind power converter (DFIG-based partial-scale and PMSG-based full-scale) is addressed and compared. Regarding the DFIG system, the injection of the reactive power from the rotor-side converter is proven a better choice due to more reactive power supply ability and less additional current stress.

According to the German grid codes, for the PMSG system, it will dissipate slightly more power loss in grid-side converter whatever the under-excited or over-excited reactive power is introduced. For the DFIG system, the influence on the power loss in rotor-side converter will be a little heavier in over-excited but even lower in under-excited than normal condition.

Based on the thermal information of the power device, along with the widely used lifetime Coffin-Manson model, it is noted that the introduction of the reactive power will also shorten the lifetime of the wind power converter significantly.

7. Literature

[1] European Commission Climate Action, "The EU climate and energy package," Mar. 2007.
[2] F. Blaabjerg, Z. Chen, S.B. Kjaer, "Power electronics as efficient interface in dispersed power generation systems," IEEE Trans. on Power Electronics, vol.19, no.5, pp. 1184-1194, Sep. 2004.
[3] F. Blaabjerg, K. Ma, D. Zhou, "Power electronics and reliability in renewable energy systems," in Proc. of ISIE'2012, pp.19-30, May. 2012.
[4] S. Yang, A. Bryant, P. Mawby, D. Xiang, L. Ran, P. Tavner, "An industrial-based survey of reliability in power electronic converters," IEEE Trans. on Industrial Applications, vol.47, no.3, pp. 1441-1451, May. 2011.
[5] E.ON-Netz. Requirements for offshore grid connections, Apr. 2008.
[6] M. Liserre, R. Cárdenas, M. Molinas, J. Rodriguez, "Overview of multi-MW wind turbines and wind parks," IEEE Trans. on Industrial Electronics, vol.58, no.4, pp.1081-1095, Apr. 2011.
[7] K. Xie, Z. Jiang, W. Li, "Effect of wind speed on wind turbine power converter reliability," IEEE Trans. on Energy Conversion, vol.27, no.1, pp.96-104, Mar. 2012.
[8] D. Zhou, F. Blaabjerg, M. Lau, M. Tonnes, "Thermal analysis of multi-MW two-level wind power converter," in Proc. of IECON'2012, pp. pp.5862-5868, Oct. 2012.
[9] User manual of PLECS blockset version 3.2.7 March 2011. (Available: http://www.plexim.com/files/plecsmanual.pdf.
[10] A. Wintrich, U. Nicolai, W. Tursky, T. Reimann, Application manual power semiconductors, Semikron International, 2011, ISBN: 9783938843666.
[11] L. Wei, R. J. Kerkman, R. A. Lukaszewski, H. Lu, Z. Yuan, "Analysis of IGBT Power Cycling Capabilities Used in Doubly Fed Induction Generator Wind Power System," IEEE Trans. on Industry Applications, vol. 47, no. 4, pp. 1794-1801, Aug. 2011.
[12] I.F. Kova evi, U. Drofenik, J.W. Kolar, "New physical model for lifetime estimation of power modules," in Proc. IPEC'2010, pp. 2106-2114, Jun. 2010.
[13] ABB Application Note, Load-cycling capability of HiPaks, 2004.